Novel LTCC-potentiometric microfluidic device for biparametric analysis of organic compounds carrying plastic antibodies as ionophores: Application to sulfamethoxazole and trimethoprim

S.A.A. Almeida, E. Arasa, M. Puyol, C.S. Martinez-Cisneros, J. Alonso-Chamarro, M.C.B.S.M. Montenegro, M.G.F. Sales

ABSTRACT

Monitoring organic environmental contaminants is of crucial importance to ensure public health. This requires simple, portable and robust devices to carry out on-site analysis. For this purpose, a low- temperature co-fired ceramics (LTCC) microfluidic potentiometric device (LTCC/µPOT) was developed for the first time for an organic compound: sulfamethoxazole (SMX).

Sensory materials relied on newly designed plastic antibodies. Sol–gel, self-assembling monolayer and molecular-imprinting techniques were merged for this purpose. Silica beads were amine-modified and linked to SMX via glutaraldehyde modification. Condensation polymerization was conducted around SMX to fill the vacant spaces. SMX was removed after, leaving behind imprinted sites of complementary shape. The obtained particles were used as ionophores in plasticized PVC membranes. The most suitable membrane composition was selected in steady-state assays. Its suitability to flow analysis was verified in flow-injection studies with regular tubular electrodes.

The LTCC/µPOT device integrated a bidimensional mixer, an embedded reference electrode based on Ag/AgCl and an Ag-based contact screen-printed under a micromachined cavity of 600 µm depth. The sensing membranes were deposited over this contact and acted as indicating electrodes. Under optimum conditions, the SMX sensor displayed slopes of about -58.7 mV/decade in a range from 12.7 to 250 µg/mL, providing a detection limit of 3.85 µg/mL and a sampling throughput of 36 samples/h with a reagent consumption of 3.3 mL per sample.

The system was adjusted later to multiple analyte detection by including a second potentiomet- ric cell on the LTCC/µPOT device. No additional reference electrode was required. This concept was applied to Trimethoprim (TMP), always administered concomitantly with sulphonamide drugs, and tested in fish-farming waters. The biparametric microanalyzer displayed Nernstian behaviour, with aver- age slopes -54.7 (SMX) and $+57.8$ (TMP) mV/decade. To demonstrate the microanalyzer capabilities for real applications, it was successfully applied to single and simultaneous determination of SMX and TMP in aquaculture waters.

1. Introduction

The (bio)analytical chemistry field needs miniature and portable analytical devices for on-site control of several compounds. In this context, flow methods with potentiometric detection are an advantageous combination. Simple flow assemblies are capable of automatic sample collection and carry out most classical analyt- ical procedures in-line, while potentiometric detectors are easily adapted to flowing media and small size sensory surfaces. This combination in microsize dimensions may produce a lab-on-a-chip device.

The introduction of micropotentiometric (µPOT) systems in analytical procedures relies mostly on solid conductive materi- als coated by ion-selective membranes. *Nernstian* responses are obtained when the analyte is the only major ion that is selectively transferred across the interface between sample and membrane

phases. In general, the selectivity is achieved by doping the membranes with a hydrophobic ion (ionic site) and a hydrophobic ligand (ionophore or neutral/charged carrier) that selectively and reversibly forms complexes with the analyte (Amemiya, 2007).

A good ligand should selectively bind the analyte and remain in the membrane phase, i.e., it should have binding sites for SMX and low water solubility. Molecularly imprinted polymers (MIPs) are a route to obtain such materials and have been introduced successfully in polymeric membranes (Kamel et al., 2008; Moreira et al., 2010). They are specifically designed to display stereochemical interactions with the analyte and act similarly to natural antibodies. They are prepared by growing a reticulated polymer around the analyte and removing the entrapped molecules later. The vacant sites are complementary to the imprinted analyte and able to rebind it. Many imprinting techniques may be employed to create MIP materials. Surface-imprinting ensures a layer-by-layer control (Moreira et al., 2011), offering a higher number of binding sites *per* contact area.

There are not many ways to introduce a μPOT sensor in a microfluidic device. Basically, it should include a solid conductive contact to apply the selective membrane, a reference electrode and microchannels driving the fluids through the sensory surfaces. Ideally, it should also carry out in-line all necessary operations to turn out a successful candidate to a Lab-on-a-chip device.

The low temperature co-fired ceramic (LTCC) technology is a possible receptor of μPOT sensor. It is a well-established technique for microfabrication (Ibañez-Garcia et al., 2008; Budniewski et al., 2004; Chou et al., 2002; Gongora-Rubio et al., 2003; Golonka et al., 2003), producing three-dimensional (3D) structures using a multi-layer approach. The LTCC devices offer good electrical and mechanical properties, as well as high reliability and stability. They may integrate in a single unit all steps associated to an analytical procedure, being of special interest to micro-fluidic applications (Golonka et al., 2006; Lopes et al., 2007; Khanna et al., 2005; Patel et al., 2006; Bergstedt and Persson, 2002; Muller et al., 2005; Zawada, 2006) and lab-on-a-chip devices.

The integration of μPOT sensors on LTCC platforms has been successfully proven in the past, although only a few works are reported. These include nitrate and chloride determinations (Ibañez-Garcia et al., 2006, 2010). However, no organic compounds have been yet considered. One of the most critical steps regarding the membrane integration to the ceramic device resides on its adhesion to the solid contact screen-printed on the ceramic surface. Therefore, additional efforts should be performed to obtain an appropriate structure to place the membrane. Moreover, these devices may last for a long time if a deteriorated selective membrane may be replaced by a new one.

In this work, the construction and evaluation of a compact LTCC/μPOT system is proposed for the on-site determination of an organic environmental contaminant. Sulfamethoxazole (SMX) has been selected as target analyte because of its environmental spread (along with other antibiotics) is becoming of great danger to public health. It has been used for long as veterinary/human antibiotic and has been found in waters, coming from municipal wastewaters and fish farming practices (Hirsch et al., 1999). A new MIP-based ligand was designed to act as SMX ionophore, as no previous MIP sensor was reported earlier. Silica beads have been modified for this purpose by surface imprinting and included in polymeric selective membranes. The optimized composition was selected after steady-state assays and dropped on tubular electrodes (for testing the membrane suitability to flow-readings) and on LTCC devices (to set operational microfluidic conditions).

Since SMX is always used in conjunction with trimethoprim (TMP), the setup was adjusted to allow the simultaneous determination of SMX and TMP. A previously reported MIP-based sensor for TMP was used for this purpose.

2. **Experimental**

2.1. *Apparatus*

EMF in steady-state assays was measured by a Crison pH-meter GLP 21 (± 0.1 mV sensitivity), at room temperature, and under constant stirring. The output signal was transferred to a home-made commutation unit with six ways out. The reference electrode was a Crison, 5240, of double-junction.

The flow setup consisted of a peristaltic pump (Minipuls 3, Gilson, WI) fitted with Tygon tubing (0.64 and 1.14 mm i.d.) purchased by Ismatec (Zurich, Switzerland). A six-port distribution valve (Hamilton, MVP, Reno, NV) of variable injection volumes was used. The several components were joined by PTFE tubing (Omnifit, Teflon, 0.8 mm i.d.). The potentiometer was coupled to acquisition/recording signal software purchased to TMI (Barcelona, Spain).

Green tapes for LTCC were machined by a laser machine (Protolaser 200, LPKF, Laser & Electronics, Germany). A thermo-compression press (Talleres Francisco Camps, Granollers, Spain) consisting of two 250×250 mm heating plates, whose temperature was controlled by means of a probe and a resistance was used for ceramic layers lamination. The devices were sintered in a programmable box furnace (Carbolite CBCWF11/23P16, Afora, Spain) following the thermal profile recommended by the ceramics manufacturer.

Infrared spectra were collected by a Nicolet iS10 FTIR spectrometer (Thermo Scientific), coupled to an ATR (Attenuated Total Reflectance) sampling accessory of diamond contact crystal from Nicolet.

2.2. *Reagents/materials and solutions*

MilliQ water was used for reagents preparation and as carrier solution. All reagents were of analytical grade. SMX, TMP, d,l-lactic acid 85%, 3-aminophenylboronic acid (APBA), tris(hydroxymethyl)aminomethane (TRIS), aminopropyl silica (particle size 15–40 μm, mean pore size 75 Å), 4-(2-hydroxyethyl)-1-piperazineethanesulfonic acid (HEPES), tetraoctylammonium bromide (TOABr) and sodium sulphate were from Sigma. *o*-Nitrophenyloctyl ether (*o*NPOE), poly (vinyl chloride) (PVC) of high molecular weight, 3-aminopropyltrimethoxysilane (APTMS), sodium persulphate (SPS), glutaraldehyde (GLU) and oxalic acid were obtained by Fluka and tetrahydrofuran (THF) by Riedel-deHäen.

The LTCC device was fabricated with green tapes (951 PX, thickness before sintering: 254 μm) and silver based pastes (6142, 6141 and 6146), both from Du Pont.

Stock solutions of SMX and TMP were prepared in water. TMP was previously solubilised in d,l-lactic acid 85% (Sigma). Working standards were prepared by single dilution of the stock solutions in HEPES buffer (steady-state assays) or water (flow assays). SMX solutions ranged from 5×10^{-5} to 1×10^{-3} M and for TMP from 2×10^{-6} to 2×10^{-5} M. Solutions with both SMX and TMP (for biparametric readings) were prepared similarly.

All solutions were measured in 1×10^{-2} M HEPES buffer, of pH 5.4. LTCC assays required the addition of 1×10^{-4} M sodium sulphate to ensure a stable baseline signal.

2.3. *LTCC device fabrication*

The design of the device consisted on nine layers that once overlapped provided the three-dimensional structure required for this application. The fabrication process regarding LTCC-based
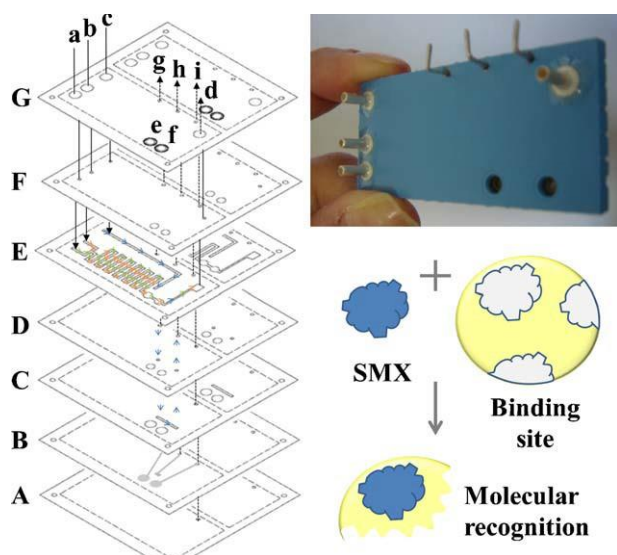
Fig. 1. Biparametric LTCC device layers (in the left; dotted lines represent the electrical contact to the external set-up and solid lines the hydraulic connections; where (a) conditioning solution inlet; (b) carrier solution; (c) KCl inlet; (d) outlet; (e) and (f) cavities for membrane deposition; (g, h) and (i) electrical connections to the external set up). Photograph of the corresponding device (top, right) and SMX recognition with the synthesized ligand (down, right).

devices is described in detail elsewhere (Ibañez-García et al., 2008). Fig. 1 presents the microanalyzer developed (2 mm height × 24 mm deep × 53 mm long), including the individual layers that integrates it. Circuit CAM software based on Windows was used to transfer the CAD layouts to the laser machine. Holes, channels, cavities and printing conductors were then mechanized on the green LTCC tapes as designed. Silver pastes were screen-printed on the correct places, to act as conductive support of all electrodes. Lamination and sintering was conducted as previously described.

The device included two liquid inlets that converged in a point downstream before getting into a bidimensional mixer. The conductive pads and their corresponding cavities for membrane deposition were defined after the mixer. The conductive pad regarding the reference electrode was defined downstream the working electrodes. The membranes were applied drop-by-drop inside the corresponding cavity, over the conductive material support, and left to dry at room temperature. Finally, hydraulic and electronic connections between the device and the external set-up were established.

2.4. Flow set-up

The conventional flow assembly consisted of a double-channel set-up, where a HEPES buffer carrier merged with a water channel transporting the injected sample. All details on electrode construction and set-up may be found in Kamel et al. (2009).

The LTCC was set-up for single (SMX or TMP) or biparametric readings (SMX and TMP together, as in Fig. 1). The carrier was always HEPES buffer with sodium sulphate and merged inside the microfluidic channels with a water channel receiving the injected samples. An auxiliary channel was used to flow 0.1 M KCl through the reference electrode to ensure its constant EMF. Single-analyte readings used a similar setup to that in Fig. 1, with only one solid contact for the selective membrane deposition.

2.5. Synthesis of the novel SMX ligand

Surface imprinting was selected to control each modification step and promote a higher number of effective binding sites.

Sol–gel, self-assembled monolayer and molecular-imprint concepts were merged in the overall procedure (Fig. 2).

About 0.1 g of silica beads (15–40 μm diameter and 75 Å pore size) were amine-modified by dipping in 10% (w/v) APTMS prepared in methanol (Fig. 2) for 1 h and washing after that (ethanol first and water later). The beads were then incubated in 1% GLU prepared in 0.01 M HEPES for 12 h at room temperature and washed after with water. The amine groups on the silica beads underwent a nucleophilic addition reaction with the aldehyde groups in GLU, forming an imine bond (–C=N–).

Then, they were dipped in 1.0 mg/mL SMX in HEPES, transferred to 1 M Tris, and thoroughly washed with water. Free-aldehyde groups from GLU on the outer layer were bound to SMX by means of the same nucleophilic addition reaction with the amine group in SMX. Tris was added after to block unreacted aldehyde functions.

Finally, the beads were dipped for 1 h in 0.05 M APBA solution prepared in water, to arrange the monomers around SMX and the amine/hydroxyl groups on the outer layer. A volume of 1 mL of 0.03 M SPS was added to initiate and carry out the polymerization for 1 h. Finally, the beads were washed again with deionised water, incubated in 1 M oxalic acid, and washed again with water. The vacant sites enabled complementary interactions with the imprinted molecule.

Non-imprinted materials (NIPs) were obtained by a similar process, where no SMX was present.

2.6. SMX and TMP selective membranes

SMX selective membranes were prepared by mixing 210 mg of PVC, 350 mg of oNPOE and 15 mg of modified silica beads (MIP or NIP). An amount of 0.2 mg of additive (TOABr) was also added to some membranes (Table 1). All these were weighted and dissolved in THF. The mixture was stirred until the PVC was well moistened. A successful TMP MIP-based sensor had already been prepared before, and was used as described by Rebelo et al. (2011).

The liquid membranes were applied over solid conductive supports and let dry for 24 h. These conductive supports were included in electrodes of conventional or tubular shape (Kamel et al., 2009) or in the microfluidic device.

2.7. Potentiometric procedures

All potentiometric measurements were carried out at room temperature. The electrochemical operating characteristics of the SMX and TMP selective electrodes were assessed after calibration curves (Buck and Cosofret, 1993) following IUPAC recommendations (Buck and Lindner, 1994). These were conducted for increasing drug concentrations in HEPES buffer 1×10^{-3} M, reaching the detector in either steady-state or flow conditions. This buffer also had 1×10^{-4} sodium sulphate in assays with the LTCC device. Potential readings were recorded after stabilization to ± 0.2 mV and plotted as a function of logarithm SMX or/and TMP concentration.

Selectivity studies followed the matched potential method for SMX assays in steady-state. The anions PO_4^{2-}, CH_3COO^-, BO_3^{3-}, CN^-, SO_4^{2-}, F^-, CO_3^{2-}, Cl^-, HCO_3^-, NO_3^-, NO_2^- and tartrate were tested for a concentration of 1×10^{-4} M. In flow conditions, selectivity was assessed by recovery assays. For this purpose, a preset drug concentration (2×10^{-4} M SMX and/or 5×10^{-6} M TMP) was spiked with different anions (NO_3^-, NO_2^-, Cl^-, HCO_3^- or SMX) or cations (K^+, $NH4^+$, Na^+ or TMP) until the maximum admitted level of each ion in water was found (excluding the drugs, to which no limit is established).
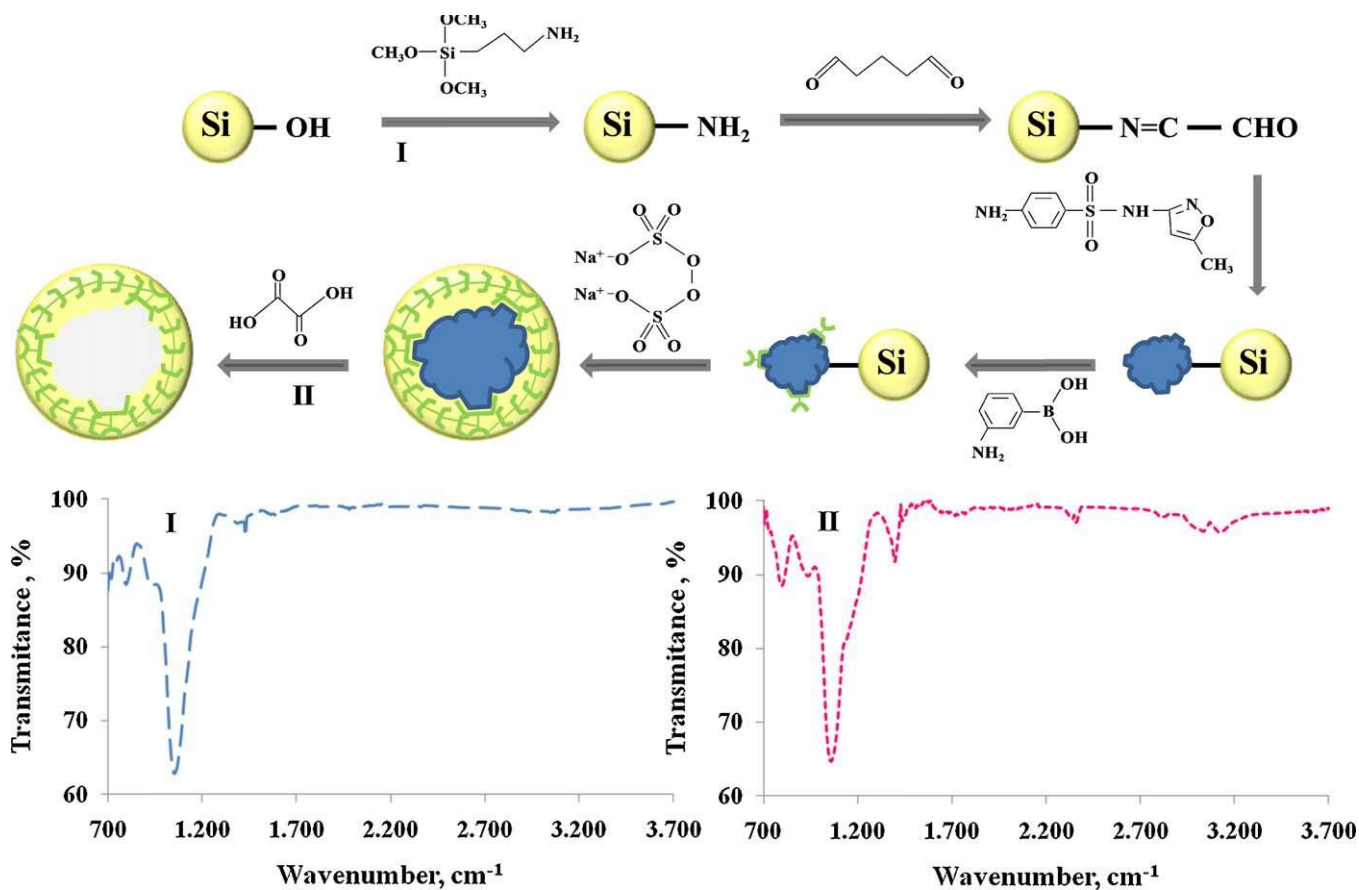
Fig. 2. Design of the plastic antibodies over silica beads and the FTIR spectra of starting and final products.

2.8. Sample analysis

Samples of aquaculture water were collected from different fish farming units in sweet waters from the north region of Portugal. The waters were not contaminated with the drugs and analysed with regard to their major organic and inorganic composition. No cation/ion was found in interfering concentrations, for which no special care was taken prior to potentiometric analysis. After, the water was spiked between 51–127 µg/mL SMX and 1.5–5.8 µg/mL TMP.

3. Results and discussions

3.1. Design control by FTIR

FTIR assays were made in all steps to control the chemical modification of the beads. The spectra of non-modified silica beads and imprinted ones are indicated in Fig. 2. Both showed significant bands at about 900 and 1100 cm^{-1}, revealing the absorption bands from the Si–OH and Si–O–Si vibrations, respectively.

Table 1
Main analytical features of all SMX and TMP sensors.

Analytical parameters	Steady-state					Flow injection			
	SMX					Tubular electrode		LTCC	
	ISE I	ISE II	ISE III	ISE IV	ISE V	ISE I	TMP	ISE I	TMP
Sensing material	MIP/SMX	MIP/SMX	NIP	NIP	–	MIP/SMX	–	MIP/SMX	–
Additive	TOABr	–	TOABr	–	TOABr	TOABr	–	TOABr	–
Plasticizer	oNPOE	oNPOE	oNPOE	oNPOE	oNPOE	oNPOE	–	oNPOE	–
Slope, mV/decade	−56.1 ± 0.2	−46.8 ± 2.0	−43.6 ± 0.7	−31.0 ± 1.7	−34.0 ± 0.8	−61.7 ± 1.4	58.7 ± 0.5	−58.7 ± 0.2	61.2 ± 0.2
R^2 (n = 3)	0.992	0.995	0.998	0.996	0.994	0.999	0.998	0.999	0.997
LLLR, µg/mL	5.49	16.2	18.9	34.9	35.4	12.7	0.290	12.7	0.580
LOD, µg/mL	1.66	4.92	5.73	10.6	10.7	3.85	0.0879	3.85	0.176
Cv$_w$ (%)	0.41	4.26	1.50	5.67	2.26	2.28	0.815	0.358	0.370
Accuracy, %	5.11	20.9	26.3	47.6	42.5	4.29	0.778	3.31	3.45
Within-day variability, %	2.77	0.802	1.53	0.46	2.19	1.76	0.983	1.25	1.17
Between-day variability, %	2.15	1.17	2.10	0.766	1.73	1.86	1.13	0.979	1.04
Recovery, %	92.7	97.1	95.1	104	101	98.4	99.0	98.4	96.3
Repeatability RSD (%)[a]	–	–	–	–	–	1.21	1.38	1.42	1.29

LOD, limit of detection; LLLR, lower limit of linear range; R^2, squared correlation coefficient; RSD, relative standard deviation; Cvw, reproducibility.

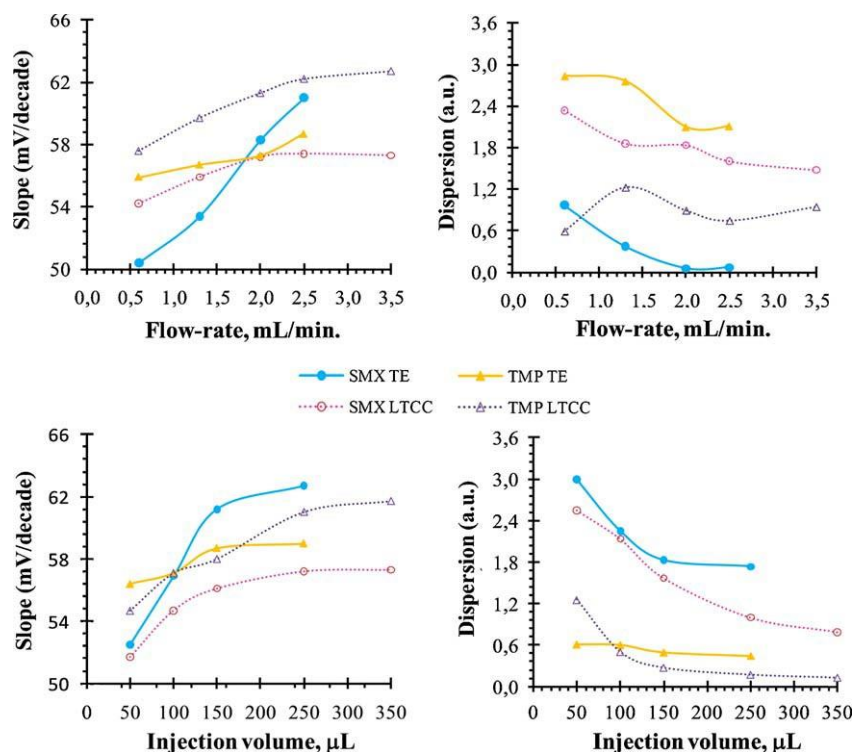[a] n = 10 for 5×10^{-6} to 5×10^{-4} M.

Fig. 3. Slope and dispersion values against injection volume and flow-rate, obtained with the tubular electrodes (TE) and the single LTCC/µPOT device.

The FTIR spectra of the imprinted beads showed specific peaks that confirmed the chemical modification of the Si–O core. The N–H bending of the secondary amines was evidenced by the small intensity peak at $1450\,cm^{-1}$. Two small peaks centered on $3000\,cm^{-1}$ evidenced the C–H stretch from bonded GLU and APBA monomer molecules.

No chemical differences were observed between the spectra of NIP and MIP beads. This was already expected because FTIR is unable to detect stereochemical differences between equivalent materials. If any chemical difference was observed that would only be attributed to template molecules trapped inside the imprinted cavities.

3.2. Selection of SMX membrane composition

The effect of using MIP materials was tested by preparing electrodes with the imprinted/non-imprinted particles acting as ionophores (Table 1). MIP-based sensors (ISE II) displayed linear responses after $16.2\,\mu g/mL$, average anionic slopes of $-46.8\,mV/decade$ and detection limits of $4.92\,\mu g/mL$. The corresponding NIP sensors were unable to reach such performance, as may be seen in Table 1. The slope was much smaller and linearity was observed only for higher concentration ranges.

MIP/NIP sensors were also prepared with TOABr (ISEs I and III). It acted as cationic additive and improved the permselectivity of the membrane. In general, the additive was fundamental to obtain Nernstian responses with MIP-based sensors ($-56.1\,mV/decade$). Improvements in limit of detection and linear range were also observed. Moreover, these ISEs displayed the best precision and accuracy features of all. The additive alone was not responsible for these improvements, considering the performance of ISEs III and V (Table 1).

The selectivity was assessed by calculating potentiometric selectivity coefficients against many (in)organic ions (Section 2.7). Log K^{POT} were < -1.0 and the relative order of interference was, $BO_3^{3-} < CO_3^{2-} \approx SO_4^{2-} < F^- < HCO_3^- < Cl^- < PO_4^{3-} <$

$CH_3COO^- \approx CN^- < NO_2^- <$ tartrate $< NO_3^-$. As expected, a deviation from the Hofmeister pattern was observed, confirming that the selectivity was not governed by ion-extraction. In general, the MIP-based sensors were more selective than NIP ones for HCO_3^-, CO_3^{2-} and Cl^-. The other tested species did not provide significant differences on the behaviour of the electrodes. The additive generated a slight improvement in the observed selectivity.

The membrane in ISE I was selected for further testing. It was applied first on tubular electrodes to check its suitability for flow experiments and after in the LTCC devices to optimize the performance under microfluidic conditions. TMP based MIP membranes were always evaluated in parallel, aiming a biparametric analysis with the LTCC/µPOT.

3.3. SMX and TMP in tubular electrodes

3.3.1. Selection of flow variables

There are only two variables deserving attention in flow-injection potentiometric systems: injection volume and flow-rate. Injection volumes were varied within 50 and 250 µL while flow-rates ranged 0.6 and 3.5 mL/min. This study was carried out by univariant mode, starting by the injection volume selection. The slope and the signal dispersion were recorded for each condition tested (Fig. 3).

In general terms, increasing the injected volume up to 150 µL lead to higher peaks and higher slopes. The sensitivity increased about 2.5% and 0.5% by changing the injection volume from 50 µL to 150 µL, for SMX and TMP, respectively. Injecting more than 150 µL produced a slight slope increase but reduced sampling-rates and almost doubled reagent/sample costs and volume of generated wastes (Yang et al., 1998). The flow-rate displayed a similar effect because only low values were tested (above 3.5 mL/min flow-rates become unsuitable for microfluidic operations). A volume of 2.5 mL/min was selected as it gave the highest sensitivity.
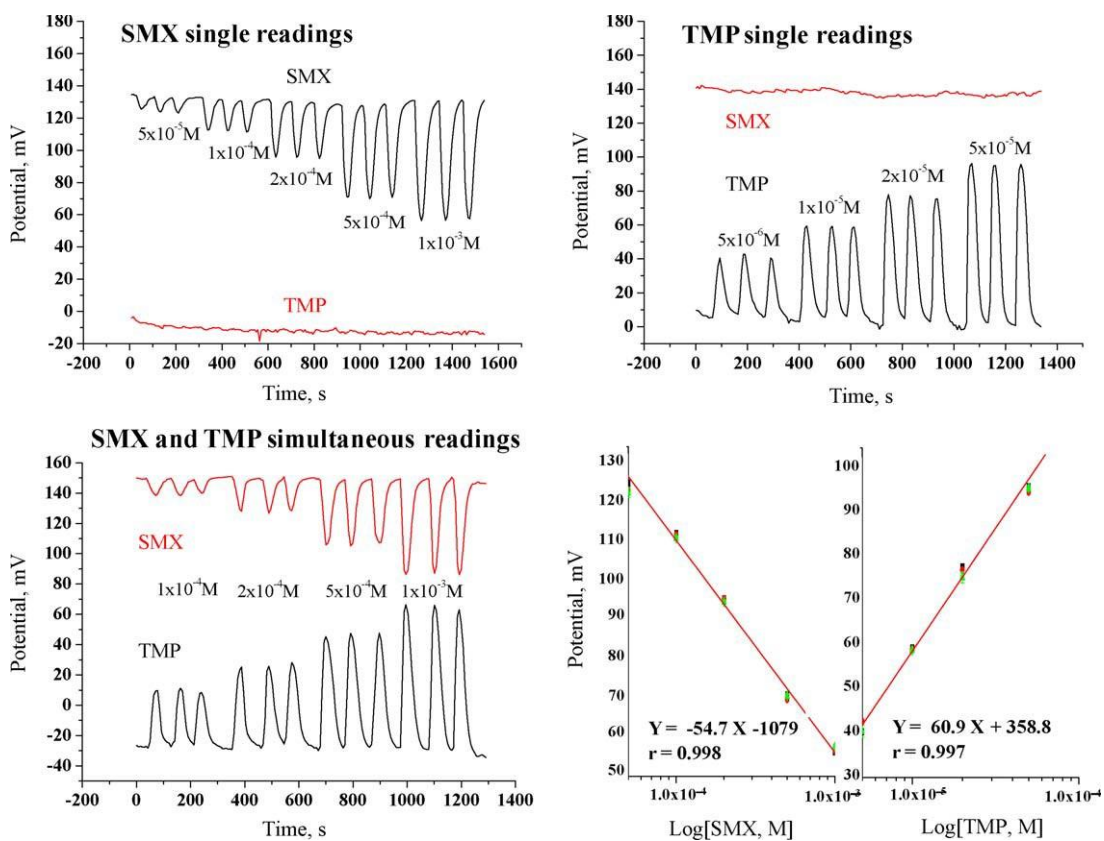
Fig. 4. Calibration of the biparametric LTCC/μPOT device with single and mixed solutions of SMX and TMP.

3.3.2. Analytical performance

SMX and TMP tubular electrodes were tested independently in conventional flow-injection setups operating with the previously established conditions. The results obtained are listed in Table 1. Linear dynamic responses ranged 5×10^{-5}–1×10^{-3} (12.7–253 μg/mL) and 1×10^{-6}–5×10^{-5} (0.290–14.5 μg/mL) M with average slopes of -61.7 and 58.7 mV/decade for SMX and TMP, respectively. The corresponding detection limits were 1.7×10^{-5} and 3.0×10^{-7} M. The repeatability of the analytical signal was assessed by injecting consecutively ten standard solutions. The relative standard deviation (RSD) was always below 1.5% (Table 1).

When SMX was added of other anionic interferences, the signal changed only slightly. NO_3^-, NO_2^- and Cl^- decrease the EMF while SO_4^{2-} increased it. A similar behaviour was observed for TMP. NH_4^+ and K^+ increased slightly the peak while Na^+ decreased it. The relative errors in terms of concentration were always below 5% for interfering concentrations up to 2×10^{-5} M.

3.4. SMX and TMP in single LTCC/μPOT

3.4.1. Set-up and LTCC design

LTCC platforms have 3D structures created by overlapping ceramic layers. Thus, the number of layers, the maximum dimensions of the device, the retraction of the materials in use and the resolution of the equipment involved were carefully considered before designing the device.

To define an optimum structure of the microanalyzer, different configurations of the detection chamber were tested. A wall-jet configuration was evaluated as a first approach. Nevertheless, in this case a brief lifetime was observed. To overcome this issue, a planar configuration, where the solutions were parallel pumped along the surface of the membrane was tried. This configuration was more suitable in terms of electrical noise and membrane adherence to the ceramic surface during longer periods of time.

The detection chamber in layer C (Fig. 1) was made larger than that in layer D. This way, when the membrane solution was applied it flew through the layer below, promoting its retention to the conductive support and avoiding liquid leakages to the latter.

The hydrodynamic parameters (flow-rate and injection volume) were optimized in the LTCC/μPOT device. The optimization was carried out in a multivariate mode, by checking the analytical signals produced after injecting 50, 100, 150, 250 and 350 μL sampling volumes, against carrier streams of 0.5, 1.3, 2.0, 2.5 and 3.5 mL/min flow rates. EMFs were evaluated in terms of dispersion and slope (Fig. 3). The best compromise was found by injecting 250 μL flowing at 2.0 mL/min.

3.4.2. Analytical performance

SMX and TMP LTCC/μPOT devices were tested independently, using the previously selected conditions. The results obtained are listed in Table 1 and indicated similar performance to that observed with the tubular electrodes. SMX μPOT showed a linear dynamic response range from 5×10^{-5} to 1×10^{-3} M (12.7–253 μg/mL) with a slope of -58.7 mV/decade and TMP μPOT from 2×10^{-6} to 5×10^{-5} M (0.580–14.5 μg/mL) with a slope of 61.2 mV/decade. The corresponding detection limits were 1.5×10^{-5} and 6.1×10^{-7} M. The selectivity behaviour was also equivalent to that observed with the corresponding tubular electrodes.

3.5. SMX and TMP in biparametric LTCC/μPOT

The calibration graphs obtained by injecting single solutions on the biparamatric system are shown in Fig. 4(top). Essentially, the analytical performance remained the same as that observed

Table 2
Results obtained by LTCC/µPOT and tubular electrodes (TE) in the determination of SMX and/or TMP in aquaculture waters.

Sample	SMX single readings					TMP single readings					SMX and TMP together[a]				
	Taken (µg/mL)	Found (µg/mL)		Recovery (%)		Taken (µg/mL)	Found (µg/mL)		Recovery (%)		Taken (µg/mL)	Found (µg/mL)		Recovery (%)	
		TE	LTCC	TE	LTCC		TE	LTCC	TE	LTCC		SMX	TMP	SMX	TMP
1	50.7	49.2	49.7	97.2	98.1	1.5	1.4	1.3	94.0	91.4	50.7	51.3	56.3	101.3	96.9
	126.7	131.7	130.2	104.0	102.8	5.8	6.1	5.9	105.0	101.3	126.7	125.8	144.8	99.3	99.7
2	50.7	48.9	50.9	96.6	100.5	1.5	1.4	1.3	94.0	91.5	50.7	47.9	57.9	94.6	99.7
	126.7	131.0	123.2	103.5	97.3	5.8	5.9	6.0	101.6	102.8	126.7	128.1	145.7	101.1	100.3
3	50.7	48.2	48.9	95.1	96.6	1.5	1.4	1.3	94.5	92.2	50.7	50.3	56.9	99.3	97.9
	126.7	126.4	127.0	99.8	100.3	5.8	5.9	5.7	101.3	98.8	126.7	127.1	146.1	100.4	100.6

[a] Biparametric LTCC/µPOT device.

for SMX and TMP solutions in the single LTCC/µPOT plafform. The sampling-rates were about 36 injections per hour and Nernstian slopes were observed (Fig. 3).

The signals obtained by injecting mixed solutions are indicated in Fig. 4. The average slope and the detection limits were −54.7 and 57.8 mV/decade, and 3.0×10^{-5} and 1.5×10^{-5} M for SMX and TMP, respectively. While SMX showed a similar behaviour, some changes were observed for TMP readings. This small cross-interference of SMX on TMP was found irrelevant because the accuracy of the EMF was ensured under this condition. Recovery values of single standard solutions lied within 95% and 101%, with relative standard deviations below 4%.

3.6. Analytical application

The flow set-ups were used to determine SMX and TMP in aquaculture waters. This was carried out with all flow set-ups established: tubular electrodes and single/biparametric LTCC/µPOT devices. The obtained results are summarized in Table 2 and correspond to the mean of at least 3 independent determinations. The standard deviations were always below 9%.

A good agreement was found between added and found amounts of the antibiotics. For single readings, the results showed recoveries ranging from 95% to 104% for SMX and from 93% to 104% to TMP. The t-student test indicated no statistical differences between the means of found amounts with tubular electrodes and LTCC devices. The p value was 0.68 for SMX and 0.38 for TMP, in both cases below the critical value (2.57).

The results obtained by the biparametric LTCC/µPOT devices were comparable to those provided by the tubular electrodes. The mean recoveries ranged from 94% to 105% and 91% to 103% for SMX and TMP, respectively. Considering as null hypothesis that the two configurations agree, a paired two-tail test for 5% level of significance gave a calculated $t(p = 0.56$ and $p = 0.15$, for SMX and TMP, respectively) below the tabulated one (2.57), therefore accepting the null hypothesis.

4. Conclusions

A new SMX ligand was successfully introduced as an ionophore in potentiometric transduction. The imprinting process was successful as the non-imprinted materials were not able to produce a Nernstian response, not even when a cationic lipophilic additive was included in the selective membrane.

A novel biparametric microfluidic potentiometric device based on the LTCC technology is developed and successfully tested to determine simultaneously SMX and TMP. SMX and TMP imprinted materials presented good behaviour in flow conditions, both in conventional tubular electrodes and in LTCC/µPOT. Biparamattic readings were enabled with little cross-interference playing no effect upon the analytical application. A sampling throughput of 36 samples per hour was achieved with the LTCC/µPOT device, producing about 4.2 mL of wastewaters *per* biparametric determination.

The biparametric LTCC/µPOT device is a good approach to a Lab-on-a-chip tool to carry out in-field analysis and simultaneous determination of SMX (or eventually other sulphonamide) and TMP.

References

Amemiya, S., 2007. In: Zoski, C.G. (Ed.), Chapter 7 in Handbook of Electrochemistry. Elsevier.
Bergstedt, L., Persson, K., 2002. Microelectron, 29.
Buck, R.P., Cosofret, V.V., 1993. Pure Appl. Chem. 65, 1849–1858.
Buck, R.P., Lindner, E., 1994. Pure Appl. Chem. 66, 2527–2536.
Budniewski, K., Golonka, L.J., Roguszczak, H., Zawada, T., Dobosz, T., 2004. Proceeding VI Optoelectronic and Electronic Sensors Conference , Wroclaw, pp. 90–93.
Chou, C.F., Changrani, R., Roberts, P., Sadler, D., Burdon, J., Zenhausern, F., Lin, S., Mulholland, A., Swami, N., Terbrueggen, R., 2002. Microelectron. Eng. 61/62, 921–925.
Golonka, L.J., Zawada, T., Radojewski, J., Roguszczak, H., Stefanow, M., 2006. Int. J. Appl. Ceram. Technol. 3, 150–156.
Golonka, L.J., Dziedzic, A., Dziuban, J., Kita, J., Zawada, T., 2003. Proceeding of SPIE on Optoelectronic and Electronic Sensors V, vol. 5124 , pp. 115–119.
Gongora-Rubio, M.R., Fontes, M.B.A., Rocha, Z.M., Richter, E., Angnes, L., 2003. Proceeding of the Eurosensors XVII , pp. 823–826.
Hirsch, R., Ternes, T., Haberer, K., Kratz, K.L., 1999. The Sci. Tot. Environ. 225, 109–118.
Ibañez-Garcia, N., Baeza, M., Puyol, M., Goméz, R., Batlle, M., Chamarro, J.A., 2010. Electroanalysis 20, 2376–2382.
Ibañez-García, N., Martinez-Cisneros, C.S., Valdes, F., Alonso, J., 2008. TRAC-Trends Anal. Chem. 27, 24–33.
Ibañez-Garcia, N., Mercader, M.B., Rocha, Z.M., Seabra, A.C., Gongora-Rubio, M.R., Chamarro, J.A., 2006. Anal. Chem. 78, 2985–2992.
Kamel, A.H., Moreira, F.T.C., Almeida, S.A.A., Sales, M.G.F., 2008. Electroanalysis 20, 194–202.
Kamel, H.A., Almeida, S.A.A., Sales, M.G.F., Moreira, F.T.C., 2009. Anal. Sci. 25, 365–371.
Khanna, P.K., Hornbostel, B., Burgard, M., Schafer, W., Dorner, J., 2005. Mater. Chem. Phys. 89, 72–79.
Lopes, X., Ibanez-Garcia, N., Alegret, S., Chamarro, J.A., 2007. Anal. Chem. 79, 3662–3666.
Moreira, F.T.C., Dutra, R.A.F., Noronha, J.P.C., Sales, M.G.F., 2011. Biosens. Bioelect. 26, 4760–4766.
Moreira, F.T.C., Kamel, A.H., Guerreiro, J.R.L., Sales, M.G.F., 2010. Biosens. Bioelectron. 26, 566–574.
Muller, E., Bartnitzek, T., Bechtold, F., Pawlowski, B., Rohte, P., Ehrt, R., Heymel, A., Weiland, E., Schroter, T., Schundau, S., Kaschlik, K., 2005. Proc. 1st Int. Conf. and Exhibition on Ceramic Interconnect and Ceramic Microsystems Technologies , Baltimore, USA, pp. 53–58.
Patel, K., Peterson, K.A., Hukari, K., 2006. J. Microelectron. Electr. Pack. 3, 152–158.
Rebelo, T.S.C.R., Almeida, S.A.A., Guerreiro, J.R.L., Montenegro, M.C.B.S.M., Sales, M.G.F., 2011. Microchem. J. 98, 21–28.
Yang, X., Hibbert, D.B., Alexander, P.W., 1998. Anal. Chim. Acta 372, 387–398.
Zawada, T., 2006. Microelectron. J. 37, 340–352.